Electrochemistry Communications 34 (2013) 228–230

Contents lists available at ScienceDirect

Electrochemistry Communications

journal homepage: www.elsevier.com/locate/elecom

Short communication

A novel bifunctional oxygen GDE for alkaline secondary batteries

Xiaohong Li [a,*], Derek Pletcher [b], Andrea E. Russell [b], Frank C. Walsh [a], Richard G.A. Wills [a], Scott F. Gorman [a], Stephen W.T. Price [b], Stephen J. Thompson [b]

[a] Energy Technology Group, Faculty of Engineering and the Environment, University of Southampton, Southampton, SO17 1BJ, UK
[b] School of Chemistry, Faculty of Natural and Environmental Sciences, University of Southampton, Southampton, SO17 1BJ, UK

ARTICLE INFO

Article history:
Received 6 June 2013
Received in revised form 24 June 2013
Accepted 25 June 2013
Available online 1 July 2013

Keywords:
Bifunctional electrocatalyst
Oxygen evolution/reduction
Gas diffusion electrode (GDE)

ABSTRACT

This paper describes a novel procedure for the fabrication of a gas diffusion electrode (GDE) suitable for use as a bifunctional oxygen electrode in alkaline secondary batteries. The electrode is fabricated by pre-forming a PTFE-bonded nickel powder layer on a nickel foam substrate followed by deposition of $NiCo_2O_4$ spinel electrocatalyst by dip coating in a nitrate solution and thermal decomposition. The carbon-free composition avoids concerns over carbon corrosion at the potentials for oxygen evolution. The electrode shows acceptable overpotentials for both oxygen evolution and oxygen reduction at current densities up to 100 mA cm^{-2}. Stable performance during >100 successive, 1 h oxygen reduction/evolution cycles at a current density of 20 mA cm^{-2} in 8 M NaOH at 333 K was achieved.

1. Introduction

Presently, there is considerable interest in rechargeable metal/air and regenerative O_2/H_2 fuel cells with alkaline electrolytes [1–4]. These require GDEs able to operate at high current densities with acceptable overpotentials and to be stable in conditions of both oxygen evolution and oxygen reduction. They should be based on non-precious metal catalysts and carbon components need to be avoided since they have a tendency to corrode when evolving oxygen. While there is substantial literature on bifunctional oxygen electrocatalysts [5–7], it generally considers only low current densities. In addition, early work [8–10] on ways to fabricate these electrocatalysts into GDEs has not been followed up. This paper therefore describes a novel approach to the fabrication of a GDE for secondary alkaline flow batteries and reports performance at high current densities.

Nickel materials are generally stable under the conditions for oxygen evolution, and hence the aim was to base all components of the GDE on such materials. The $NiCo_2O_4$ spinel was selected as the bifunctional electrocatalyst since it is known to be an effective catalyst for both O_2 reduction and O_2 evolution [5,10–15], and preliminary studies showed it to be an effective catalyst. It was also simpler to prepare than other oxide catalysts and the relatively low temperature for its preparation is critical to the procedure used for fabrication of the GDE.

2. Experimental

Nickel powder (Huizhou Wallyking Battery Ltd, 2–10 μm particle size by SEM), nickel foam (Goodfellow, thickness 1.6 mm, 20 pores/cm), nickel nitrate (Aldrich, 99.999%), cobalt(II) nitrate (Aldrich, ≥ 98%), sodium hydroxide (Fisher, 97%), polytetrafluoroethylene (PTFE, Aldrich, 60 wt% dispersion in H_2O), and commercial Pt/carbon GDEs (Johnson Matthey Fuel Cells, 15 wt % Pt with loading 4 mg cm^{-2}) were used as received.

The procedure for making the bifunctional oxygen electrodes had two stages. The first stage led to a porous nickel powder/PTFE layer on nickel foam. Nickel foam (70 mm × 120 mm) was cleaned by sonicating in isopropanol and then water for 15 min each. Nickel powder and PTFE binder (solid weight ratio 10 to 3) were mixed with isopropanol and water to form an ink then dried to a paste. The paste (loading ≈150 mg cm^{-2}) was spread uniformly on the nickel foam giving a paste area of 50 mm × 100 mm, and the structure was then compressed in a hydraulic Instron C press using 10 MPa at 298 K for 1 min. The second step was to form the catalyst layer. The nickel powder/PTFE-coated nickel foam was soaked in a solution containing 0.5 M $Ni(NO_3)_2$ and 1 M $Co(NO_3)_2$, dried at 298 K for 10 min and then heat treated in a Carbolite ELF 11/6 furnace at 648 K for 15 min to form the $NiCo_2O_4$ spinel. The dip, dry and heat cycle was repeated 6 times before the sample was calcined at 648 K for 3 h. X-ray diffraction confirmed that layers formed in this way had a spinel structure. The uniformity of the GDE structure was checked by SEM while the cross-sectional SEM images of the final GDE show its thickness to be ~1 mm. The loading by $NiCo_2O_4$ was estimated to be ~3 mg cm^{-2} by weight increase. For the experiments reported here, discs 12 mm in diameter were cut from the finished electrodes.

* Corresponding author. Tel.: +44 2380 594905; fax: +44 2380 597051.
E-mail address: Xh.Li@soton.ac.uk (X. Li).

1388-2481
http://dx.doi.org/10.1016/j.elecom.2013.06.020

Electrochemical measurements were carried out using an Autolab potentiostat/galvanostat, PGSTAT30. Most experiments used a water jacketed glass cell (volume 200 cm^3) with a GDE, a platinum gauze counter electrode and a Hg/HgO reference electrode placed inside a compartment with a Luggin capillary. The GDE was mounted inside a PTFE holder and electrical contact made with a nickel wire and mesh on the gas side. A Camlab W14 water recirculator maintained the electrolyte temperature at 333 K. O_2 was passed to the rear of the GDE with a feed rate of 200 cm^3 min^{-1}, controlled via a flowmeter. Unless otherwise stated, the electrolyte was 8 M NaOH at 333 K. Current cycling was carried out under galvanostatic control at current densities in the range 10–100 mA cm^{-2}. Current densities are based on the geometric area of the electrode (0.5 cm^2) exposed to the electrolyte and gas compartments. Some cyclic voltammetry employed a conventional three electrode cell where the $NiCo_2O_4$ spinel layer was deposited directly onto a low area, fine nickel mesh.

3. Results and discussion

Electrodes were prepared using the procedure described above. With Ni powder and PTFE on the Ni foam, but without the deposition of the $NiCo_2O_4$ coating, the electrodes showed very poor activity for O_2 reduction. When the spinel coating was deposited by dipping the preformed electrode in Ni/Co nitrate solution followed by thermal decomposition, the performance improved markedly. Fig. 1 shows the potential vs. time responses for O_2 reduction and evolution at a constant current density of 20 mA cm^{-2} for the $NiCo_2O_4$-coated GDE in 8 M NaOH at 333 K. It can be seen that the potential quickly reaches a constant value during both oxygen reduction and evolution. The steady-state potentials are separated by only 620 mV confirming that $NiCo_2O_4$ spinel is an effective bifunctional catalyst in this alkaline medium. A number of electrodes were tested with carbon powder or carbon paper components but all failed after a period of O_2 evolution when large increases in overpotential occurred, and there was visible signs of corrosion of the structure [5]. This is illustrated by data for a commercial Pt/carbon GDE. When an initial cathodic current is passed, the Pt catalyzed GDE performs well, giving a slightly lower overpotential (~40 mV) for oxygen reduction than observed with the spinel. On the other hand, after a short period of O_2 evolution, there is a catastrophic increase in potential.

Fig. 2(a) reports the performance of the $NiCo_2O_4$-coated GDE when it was cycled between oxygen reduction and oxygen evolution using a current density of 20 mA cm^{-2} for 1 h periods at 333 K. The potentials for oxygen reduction and evolution are ~−0.08 V and ~+ 0.54 V vs. Hg/HgO, respectively, giving a 620 mV potential difference between these two reactions. Moreover, there was no degradation in steady-state performance over the timescale of 100 cycles (the figure shows the first 50 cycles). In fact, there is slight trend to lower overpotential for both reactions. It was also noted that the open circuit potentials following O_2 evolution and reduction were quite different, see Fig. 3. Fig. 2(b) shows an expanded view of the potential vs. time

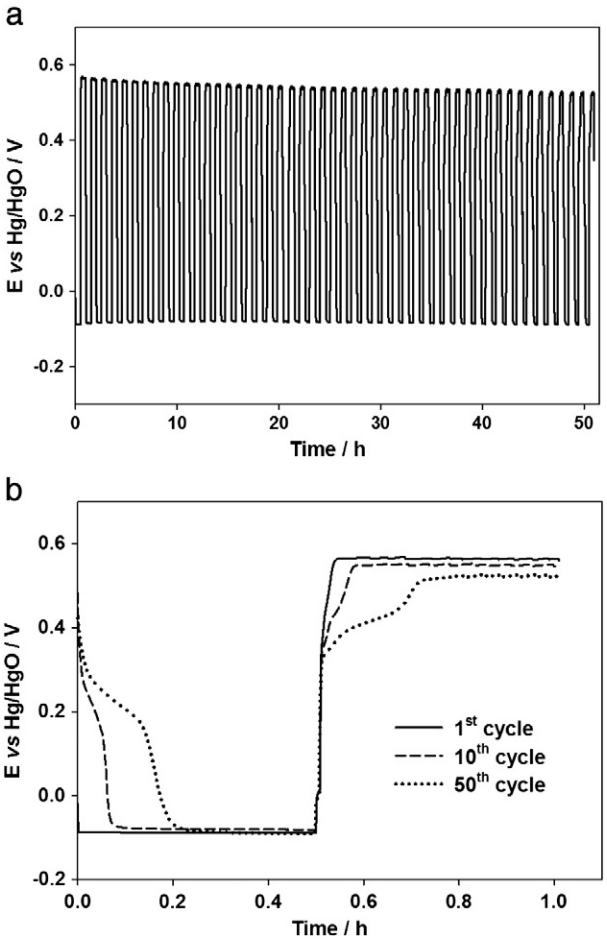

Fig. 2. (a) Potential vs. time responses during current density cycling of a spinel-coated Ni/PTFE GDE in 8 M NaOH at 333 K. Current density 20 mA cm^{-2}. Oxygen feed rate: 200 cm^3 min^{-1}. Shown are 1st to 50th cycles. Each cycle—1 h. (b). Expand presentation of the 1st, 10th and 50th cycles.

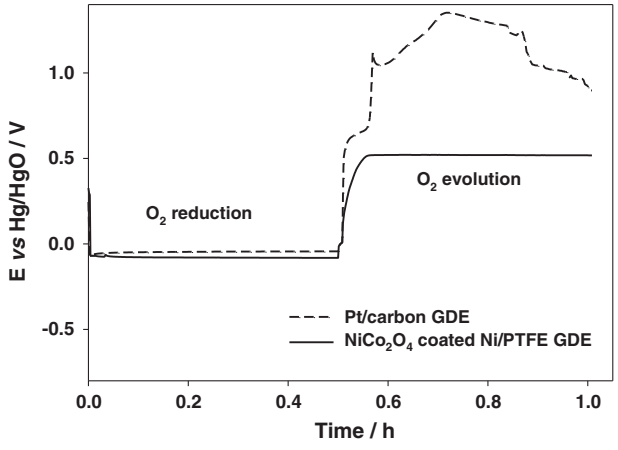

Fig. 1. Comparison of potential vs. time responses during current density cycling of spinel-coated Ni/PTFE GDE and a commercial Pt/C GDE. Cathodic and anodic currents both 20 mA cm^{-2}. Fresh GDE. Electrolyte: 8 M NaOH at 333 K. Oxygen feed rate: 200 cm^3 min^{-1}.

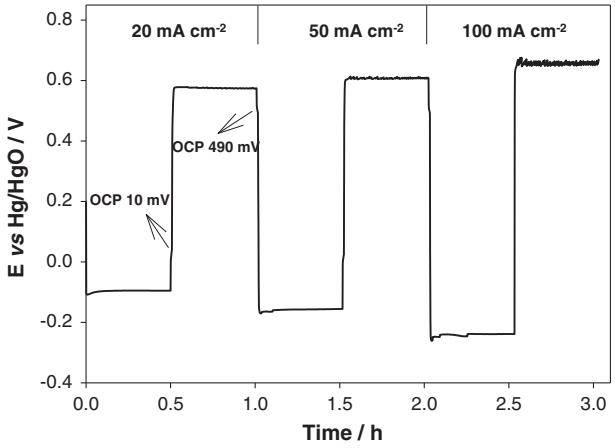

Fig. 3. Potential vs. time responses during current density cycling of a spinel-coated Ni/PTFE GDE. Current densities: 20, 50 and 100 mA cm^{-2} in 8 M NaOH at 333 K. Fresh GDE. Oxygen feed rate: 200 cm^3 min^{-1}.

responses during the 1st, 10th and 50th cycles. It can be seen that on switching between cathodic and anodic current, there is a period where the overpotentials are lower before it increases to that for oxygen reduction/evolution. On the first cycle, this period is short but it extends with cycling and eventually becomes an important component of the electrode behavior. It should be emphasized that these lower overpotential periods are beneficial since when the electrodes are used in a battery, the voltage efficiency of the battery is improved. During this period, another reaction must be occurring; this is likely to be the inter-conversion of $Ni(OH)_2$/NiO(OH) or a metal oxidation state in the spinel coating at the electrolyte/electrode interface. Since the period of lower overpotential is lengthening during cycling, it suggests that the interfacial area is increasing, e.g., there is some movement of electrolyte through the GDE structure.

The performance of the $NiCo_2O_4$-coated electrode at different current densities is shown in Fig. 3. At all current densities, stable potentials are seen during both oxygen reduction and evolution. As expected, the overpotentials for both electrode reactions increase with current density. The increases are larger than expected for the increased rate of electron transfer alone suggesting a contribution from IR drop in the electrolyte between Luggin capillary tip and the GDE as well as perhaps within the electrode itself.

In order to provide background information, some voltammograms were recorded for a small piece (~10 mm × 10 mm) of fine nickel mesh both uncoated and $NiCo_2O_4$ coated. Fig. 4 compares the voltammograms recorded at 298 K and using a potential scan rate of 50 mV s^{-1}. Both responses show oxidation/reduction peaks at potentials just negative to oxygen evolution. For the uncoated nickel, a well-formed, symmetrical anodic peak and a coupled symmetrical cathodic peak are seen. These are associated with surface conversion between $Ni(OH)_2$ and NiOOH [15–18]. With the spinel-coated electrode, the charges associated with oxidation and reduction are much higher as expected for a rough and perhaps porous coating. The response is also more complex. Three overlapping anodic peaks are seen on the forward scan at +340 mV, +460 mV and +500 mV, with the latter two peaks not well resolved and the response on the reverse scan consists of very broad peaks. The shape of the peaks and the charge balance between total anodic and total cathodic charges confirm that the electrochemistry is reversible and occurring within a surface layer. This is confirmed since there is no significant change between the 1st and the nth scan cyclic voltammograms. This voltammetry is similar to that reported by Rasiyah et al [12]. While it is not possible to assign the peaks to specific reactions, in general, there is little doubt that the peaks result from changes to the oxidation state of nickel and cobalt centres within the spinel structure. The voltammetry also shows most clearly that at the potentials for oxygen reduction and oxygen evolution, the catalyst is in different oxidation states.

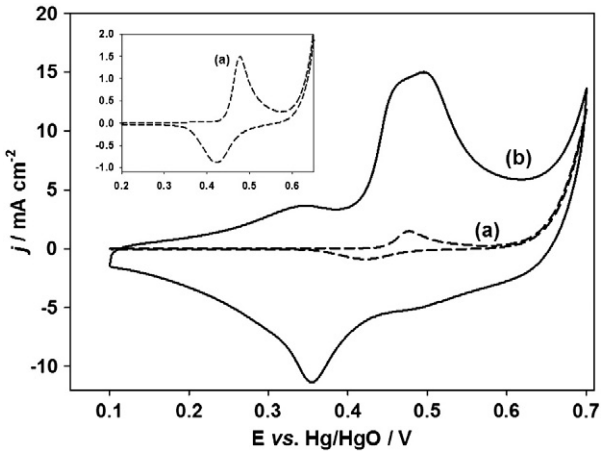

Fig. 4. Cyclic voltammograms recorded at a spinel-coated nickel mesh (b) and an uncoated nickel mesh (a) in 4 M NaOH at 298 K. Potential sweep rate: 50 mV s^{-1}. The inset shows an expanded view of the voltammogram at the uncoated mesh.

The spinel catalyzed GDE when cycled between cathodic and anodic currents must be expected to undergo the same change in metal oxidation state where there is an interface between catalyst and electrolyte. This is seen in the potential/time responses (Fig. 2(b)). Moreover, the open circuit potentials immediately after periods of oxygen reduction and oxygen evolution are quite different, + 10 mV and + 490 mV vs. Hg/HgO, respectively. Hence, (a) the two reactions are occurring on surfaces with transition metals in different oxidation states and all the oxidation states are stable, and (b) cycling between oxygen reduction and oxygen evolution requires the passage of a charge to effect this change in oxidation state before oxygen evolution/reduction can occur.

4. Conclusions

The procedure described in this paper leads to the fabrication of gas diffusion electrodes without carbon components. After the formation of a Ni powder/PTFE layer within Ni foam, the spinel catalyst layer is formed by a simple dip/heat cycle. Such GDEs performs well as a bifunctional oxygen electrode in alkaline environments. They give acceptable overpotentials for both O_2 reduction and evolution and may be extensively cycled between oxygen evolution and reduction without loss in performance. The compressed nickel foam provides both strength and good continuous electrical contact with the external circuit. The absence of precious metals and the simplicity of fabrication create the opportunity for low cost GDEs.

While details of the mechanism for these reactions have not been studied, it is interesting to note that the two reactions occur on surfaces where the transition metals are in different oxidation states. These changes in oxidation state provide a mechanism for short charges/discharges with very good energy efficiency. When these period are over, oxygen evolution/reduction take over as the electrode reactions, giving a lower voltage efficiency but giving the possibility of long timescale charge/discharge cycles.

Acknowledgements

Financial support by the European Commission (Theme 2010.7.3.1), Energy Storage Systems for Power Distribution Networks, grant agreement no. 256759, is gratefully acknowledged.

References

[1] R.P. Hamlen, T.B. Atwater, in: D. Linden, T.B. Reddy (Eds.), Handbook of Batteries, third ed., McGraw-Hill, New York, 2002, pp. 38.1–38.53.
[2] F. Cheng, J. Chen, Chemical Society Reviews 41 (2012) 2172.
[3] J.S. Lee, S.T. Kim, R. Cao, N.S. Choi, M. Liu, K.T. Lee, J. Cho, Advanced Energy Materials 1 (2011) 34.
[4] J.D. Maclay, J. Brouwer, G.S. Samuelsen, International Journal of Hydrogen Energy 31 (2006) 994.
[5] K. Kinoshita, Electrochemical Oxygen Technology, John Wiley & Sons Inc., 1992
[6] A. Cisar, M. Bryan, C. Bryan, US Patent, US 2003/0068544A1.
[7] L. Jörissen, Journal of Power Sources 155 (2006) 23.
[8] L. Öjefors, L. Carlsson, Journal of Power Sources 2 (1977/78) 296.
[9] L. Carlsson, L. Öjefors, Journal of the Electrochemical Society 127 (1980) 525.
[10] G. Karlson, H. Lindstrom, Journal of Molecular Catalysis 38 (1986) 41.
[11] M.R. Tarasevich, B.N. Efremov, in: S. Trasatti (Ed.), Electrodes of Conductive Metallic Oxides, Elsevier Scientific Publishing Company, 1980, pp. 221–259.
[12] P. Rasiyah, A.C.C. Tsueng, D.B. Hibbert, Journal of the Electrochemical Society 129 (1982) 1724.
[13] P. Rasiyah, A.C.C. Tseung, Journal of the Electrochemical Society 130 (1983) 2384.
[14] P.N. Ross, Proceedings of the 10th Annual Battery Conference on Applications and Advances, 1995, pp. 131–133.
[15] X. Li, F.C. Walsh, D. Pletcher, Physical Chemistry Chemical Physics 13 (2011) 1162.
[16] M. Fleischmann, K. Korinek, D. Pletcher, Journal of Electroanalytical Chemistry 31 (1971) 39.
[17] R.S. Schrebler Guzman, J.R. Vilche, A.J. Arvia, Journal of the Electrochemical Society 125 (1978) 1578.
[18] P.M. Robertson, Journal of Electroanalytical Chemistry 111 (1980) 97.